

Interplay between motility and cell-substratum adhesion in amoeboid cells

Xiaoying Zhu,¹ Roland Bouffanais,^{1,a)} and Dick K. P. Yue^{2,b)}

¹Singapore University of Technology and Design, 8 Somapah Road, Singapore 487372

²Massachusetts Institute of Technology, 77 Massachusetts Avenue, Cambridge, Massachusetts 02139, USA

(Received 14 June 2015; accepted 15 September 2015; published online 29 September 2015)

The effective migration of amoeboid cells requires a fine regulation of cell-substratum adhesion. These entwined processes have been shown to be regulated by a host of biophysical and biochemical cues. Here, we reveal the pivotal role played by calcium-based mechanosensation in the active regulation of adhesion resulting in a high migratory adaptability. Using mechanotactically driven *Dictyostelium discoideum* amoebae, we uncover the existence of optimal mechanosensitive conditions—corresponding to specific levels of extracellular calcium—for persistent directional migration over physicochemically different substrates. When these optimal mechanosensitive conditions are met, noticeable enhancement in cell migration directionality and speed is achieved, yet with significant differences among the different substrates. In the same narrow range of calcium concentrations that yields optimal cellular mechanosensory activity, we uncovered an absolute minimum in cell-substratum adhesion activity, for all considered substrates, with differences in adhesion strength among them amplified. The blocking of the mechanosensitive ion channels with gadolinium—i.e., the inhibition of the primary mechanosensory apparatus—hampers the active reduction in substrate adhesion, thereby leading to the same undifferentiated and drastically reduced directed migratory response. The adaptive behavioral responses of *Dictyostelium* cells sensitive to substrates with varying physicochemical properties suggest the possibility of novel surface analyses based on the mechanobiological ability of mechanosensitive and guidable cells to probe substrates at the nanometer-to-micrometer level. © 2015 AIP Publishing LLC. [<http://dx.doi.org/10.1063/1.4931762>]

I. INTRODUCTION

Amoeboid motility is a fast mode of cellular migration used by mammalian cells such as neutrophils and some metastatic cells to enter and translocate through various tissues and organs without tightly adhering to specific substrates.^{1,2} The molecular mechanisms underlying the migration of such highly motile cells have been extensively studied in the past decades,³ revealing complex physically integrated molecular processes involving biochemical cascades intercorrelated with external chemo- and mechanostimuli.⁴ Many of these studies involved the use of the lower eukaryotic amoeba *Dictyostelium discoideum*⁵ (Dd), a model organism easily amenable to genetic analysis and sharing many motile characteristics with neutrophils, lymphocytes, and some tumor cells, including chemotactic behaviors^{1,6} and mechanotactic ones.^{7–10} As an haptokinetic process, amoeboid crawling requires appropriate adhesion to the substratum so that traction can be gained, and such that the cell can move forward. With sufficient adhesion, amoeboid movement occurs from alternating cycles of cytoskeletal expansion and myosin-

^{a)}Electronic mail: bouffanais@sutd.edu.sg

^{b)}Electronic mail: yue@mit.edu

driven retraction leading to shape changes in the form of pseudopod¹ or in the form of the relatively overlooked leading-edge bleb formation.¹¹

Cellular adhesion, much like motility, is a complex, dynamic, and highly regulated process. Dynamic and coordinated changes in the actin-myosin cytoskeleton with actin polymerization at the leading edge provide the driving force for extension, and contractile forces allows the detachment and retraction of the rear end.^{12,13} Cell-substrate adhesion is an active process since cells are not adhesive *per se*. Indeed, its regulation is critical for effective cell migration. For the social amoebae *Dd*, a clear and detailed picture of the mechanisms and structures underlying cell-substratum adhesion is still lacking, although some progress has been reported over the past decade. According to Uchida and Yumura,¹⁴ *Dictyostelium's* adhesion to the substratum stems from actin foci. These very dynamic structures have been found to be the sites where traction forces are transmitted to the substrate, and thus have been proposed as likely candidates for *Dictyostelium* feet. Unlike mammalian cells, *Dictyostelium* cells are unable to form integrin-mediated focal adhesions since they lack genes encoding integrin homologs.¹⁵ However, several other transmembrane proteins have been identified to mediate adhesion in *Dd*—among others *SibA*, *SibC*, *Phg1*, *Phg2*, and *SadA*—in different growth phases and with specific substrate types.^{16–19} Recently, Loomis *et al.*²⁰ also considered the possible involvement of innate nonspecific cell-substratum adhesions, which were shown to play an important role.

The exact role of cell-substratum adhesion on *Dictyostelium's* motility is still debated, although it is well accepted that both processes are clearly interwoven.²¹ For instance, cell-substratum adhesion strength—known to be around 1 Pa for *Dictyostelium* cells⁴—has a marked biphasic effect on migration speed.¹ Hence, the effectiveness of the haptokinetic migration of amoeboid cells requires a fine balance between adhesion and de-adhesion rates. A too weak adhesion to the substrate eventually results in a loss of contact with the substrate therefore preventing active directional migration. On the other hand, a too high adhesion to the substrate yields a speed reduction as de-adhesions at the rear end are impeded.

Beyond the apparent interplay between adhesion and amoeboid motility, it is important to highlight the central role played by mechanosensitivity in both of these cellular processes. Recent studies indicate that mechanical forces have a far greater impact on cell structure and function than previously appreciated.²² For instance, eukaryotic cells such as epithelial cells,²³ amoebae,^{7,8,24} and neutrophils,¹⁰ are remarkably sensitive to shear flow direction. In the particular framework of our study, the interwoven processes of migration and adhesion are noteworthy among the many cellular processes regulated by physical forces. Recent studies have established that at the adhesion sites—where the transmembrane protein receptors form bridges with the substratum, cells can not only sense the chemical features of the substrate but also a wide range of mechanical cues.^{25,26} This includes fluid flows and shear stresses, deformations of elastic or solid materials, and a complex transfer loads between the various interacting components of the cell itself and its surrounding environment.²⁷ It is worth adding that adhesion-mediated mechanosensitivity allows cells to probe two physical aspects of their environment, namely, force and geometry at the nano-to-micrometer level,²⁸ with an effectiveness that depends on the adequate functioning of the mechanosensors as well as the chemical nature of the underlying substrate. For instance, some cells are able to display a durotactic motile behavior during which migration is oriented along the gradient of the rigidity of the substrate.²⁹ More recently, mechanical cell trapping has been achieved using specific 3D-microstructured surfaces³⁰ and fluid shear stress.⁸ These results underscore the fact that a fine control of the physicochemical features of the microenvironment^{27,31–33} should open new avenues for cell control and manipulation,^{34–36} hence paving the way for innovative applications in biotechnology and regenerative medicine.

The mechanisms underlying the conversion of mechanical signals at the adhesion sites into intracellular chemical signals are still largely obscure. A host of molecular sensors have been shown to be involved in the process of mechanotransduction, including G protein-coupled receptors in neutrophils subjected to fluid shear stress.⁹ However, mechanosensitive ion channels (MSCs) are among the most efficient mechanosensors and also the fastest acting.³⁷ They form a special group of mechanosensors that also serve the role of effectors through the

mediation of a flux of specific cations, such as Ca^{2+} , across the cellular membrane. The physical limits on cellular directional mechanosensing have been theoretically investigated in the particular case of stretch-activated MSCs,³⁸ for which the stimulus mechanically deforms the membrane's lipid bilayer, in turn triggering protein conformational changes from a closed state to an open one.³⁹ The existence of calcium-based stretch-activated MSCs in Dd was first revealed by Lombardi *et al.*⁴⁰ Very recently, Lima *et al.*⁴¹ established that the calcium-based MSC PKD2 is the major player in *Dictyostelium*'s shearotactic response,^{7,8} improved by calcium mobilization.²⁴ Indeed, PKD2 is a transmembrane protein that allows calcium influxes in response to mechanical stress or extracellular calcium changes.⁴¹ This recent discovery sheds a new light on a host of results underscoring the pivotal role played by soluble calcium on some specific behaviors of Dd. For instance, the extracellular Ca^{2+} has been shown to be a key parameter in the random motile behavior of aggregation competent cells,⁴² while also enhancing chemotactic efficiency.⁴³ Moreover, soluble calcium affects the shearotactic prowess of vegetative cells.^{8,24} Very recently, we uncovered the existence of an optimal level of extracellular calcium of 3 mM at which both speed and directionality of shearotactically driven vegetative Dd cells are maximum.⁸ Interestingly, this optimal value is very close to levels of soluble calcium commonly found in soil solutions.⁴²

The interplay between amoeboid motility, cell-substratum adhesion, and mechanosensitivity has so far been investigated only through a reductionist "paired approach," namely: (i) motility vs. adhesion,^{1,2,14,21} (ii) motility vs. mechanosensitivity,^{7,8,10,29–33,40,44} and (iii) adhesion vs. mechanosensitivity.^{9,25–27} The recent discovery of PKD2 as the primary calcium-based mechanosensor in Dd⁴¹ combined with the mounting evidence of the important effects of extracellular calcium on both migration^{8,24,40,42} and cell-substrate adhesion⁴² suggests an intricate triadic coupling between migration, adhesion, and mechanosensation. Here, we present the first investigation of this triadic coupling through a quantitative assessment of the interplay between cellular migration and adhesion using a carefully controlled mechanotactic signal in the form of fluid shear stress. Specifically, we follow the approach we reported,⁸ in which Dd cells are placed within a microfluidic cell system that allows the application of stable temporally controlled shear stresses. This system permits direct visualization of transient responses of multiply seeded cells. Within this well-controlled *in vitro* environment, multiple independent single-cell trackings can simultaneously be achieved, allowing us to obtain quantitative statistical characterizations of the shearotactically driven migration. The appropriate selection of a low mechanotactic signal shear stress ($\sigma \sim 0.2$ Pa) and the optimal calcium concentration of 3 mM led to substantially enhance directed migratory responses in terms of both speed and directionality compared to prior studies.^{7,24} However, one important element was lacking in our previous search for optimal conditions to mechanotactically drive Dd cells,⁸ namely, the influence of the nature of the underlying substratum.

In principle, the study we describe can be applied to exhaustively quantify, in terms of the directed crawling of Dd cells and the associated adhesion, substrates with (widely) different physical and chemical properties. As proof of concept, we investigate and show how the effectiveness of mechanosensation over selected different substrates influences directed migration and cell-substrate adhesion. Our results establish the central role played by mechanosensation in allowing the cell to actively select the appropriate level of adhesion resulting in the most effective directed migration possible. Specifically, we show that the directed migration of vegetative Dd cells is optimal—in terms of speed and directionality—at the same level of extracellular calcium of 3 mM, for three substrates considered (with vastly different hydrophobicities and hardness), with qualitative differences among these substrates amplified in the vicinity of this level. Coincidentally (but not surprisingly), the measure of cellular adhesion—based on the remaining fraction of a cell population subjected to a given magnitude of shear stress for a fixed duration—is found to be minimal near the same optimal level of soluble calcium of 3 mM, for all the substrates considered, again with qualitative differences among them in the adhesion measure. Finally, when cellular mechanosensation is knocked out—by blocking most stretch-activated MSCs, including the identified PKD2, using a sufficient amount of gadolinium

(Gd^{3+})—no active reduction in substrate adhesion is achieved leading to the same undifferentiated and drastically reduced level of directed migration.

Overall, these results reveal and detail for the first time the pivotal role played by mechanosensation in controlling the interplay between directed migration and cell-substrate adhesion. This fact could potentially lead to innovative applications in the field of tissue engineering and regenerative medicine if proven to be effective with mammalian cells. For instance, such responses and control of cell motility to various mechano- and chemostimuli might open new possibilities for cell sorting in surface and mechanically controlled assays.^{32,33} Moreover, these mechanobiological results suggest and could form the basis of novel means of quantifying differences among surfaces with (minor) variations in physicochemical properties. Specifically, one could use a population of mechanosensitive and shearotactically guidable cells to mechanotactically “probe” these different surfaces and to differentiate their physicochemical properties based on the cellular response to induced directed migration.

II. MATERIALS AND METHODS

A. Cell growth and preparation

Wild-type *Dictyostelium discoideum* AX2 cells (strain obtained from DictyBase; Depositor: Wolfgang Nellen) were grown at 23 °C in axenic medium (HL5) on Petri dishes.⁴⁵ Vegetative cells were harvested during the exponential growth phase with a density not exceeding 1×10^6 cells/ml, pelleted by centrifugation (1000 g, 4 min). Cells were then washed twice with MES-Na buffer (20 mM morpholinoethanesulfonic acid, adjusted to pH 6.2 with NaOH) and used immediately. For all experiments involving the blocking of stretch-activated MSCs, gadolinium hydrochloride III (Gd^{3+}) with concentrations ranging from 1 μ M to 100 μ M was added to the MES-Na buffer. To avoid any damage to cells due to even moderate exposure to light, each sample was used for less than 40 min.

Significant variability in cellular response is not uncommon with Dd, when subjected to chemo- or mechanotactic signals, as well as in the absence of any driving signal. Beyond the inherent biological variability, the environmental factors associated with the experimental conditions—growth time, buffer conditions, and cell density in particular—are at the root of such significant variability in outcome for different batches of cells. To ensure consistency in results and minimize this issue, we imposed very strict experimental operating procedures for the control of growth time, buffer conditions, and cell density. With such stringent operating conditions, most batches of cells—9 out of 10 typically—yielded statistically consistent results. The occasional “irregular” batches were easily detected (see Sec. II F) and thereby discarded.

B. Cell Motility Device Design

Shearotactic cell motility assays were conducted in an optically transparent flow chamber (Fig. 1, left) in which both the magnitude and direction of the shear stress are uniform throughout the (yx)-surface of the observation area A located at the center of the channel (Fig. 1, left), and temporally controlled using an external flow circuit connected to a syringe pump having a highly controllable flow rate. Vegetative Dd cells adherent to the bottom surface of the observation area A (Fig. 1, left) are subjected to an externally controlled shearotactic signal of very small magnitude. Their migratory responses are tracked by recording the cell trajectories, typically over a duration of 10 to 20 min, during which some cells travel over 8 to 16 times their body length—measured to be on average 14 μ m for the cell strain we considered.

Cell tracking experiments were carried out at ambient temperature (23 °C) under a Nikon Eclipse Ti-S phase contrast microscope equipped with 10 \times and 20 \times long working distance objectives and a fast camera (Nikon digital sight DS-Ri1) was used to capture the images. An area of approximately 1 mm² at the center part of each channel was used for measurement.

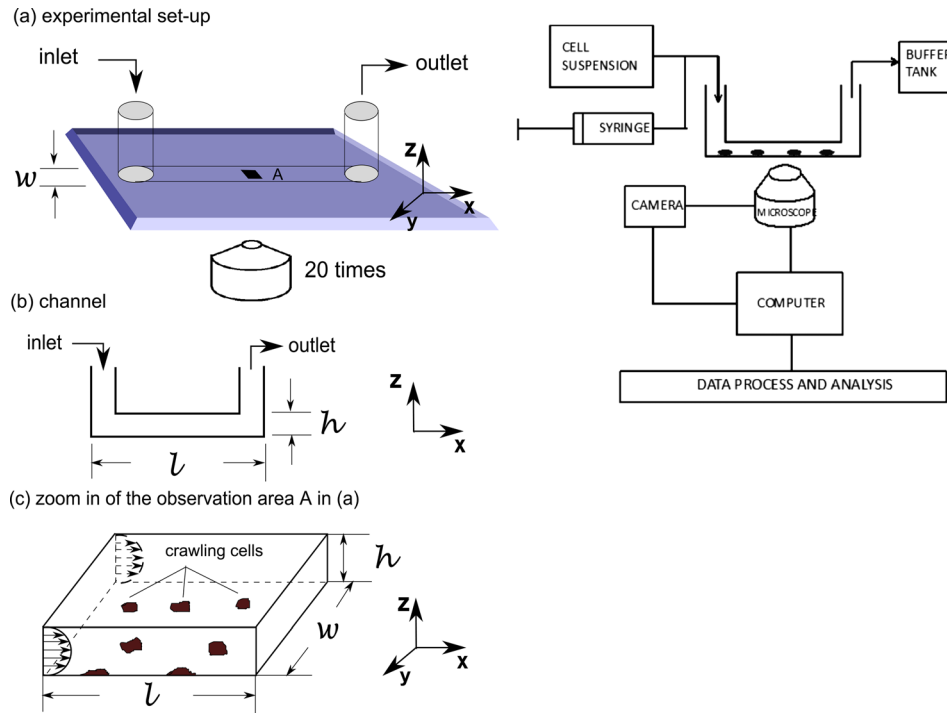


FIG. 1. (left) Schematic of the microfluidic device used to investigate the effects of shearotactic signals on cell migration and cell-substrate adhesion. The external flow circuit comprising the syringe pump is not represented but is connected to the inlet and outlet of the microfluidic channel. Different values for the channel height h , width w , and length l were considered depending on the type of channel and nature of the bottom substrate. (right) Schematic diagram of the entire experimental setup.

Data acquisition and analysis using the image processing and cell tracking software Image Premier Pro (Media Cybernetics MD) were as described in Ref. 8.

A dual-rate syringe pump (KDS) was used to generate continuous creeping flows with a flow rate ranging from 0.1 ml/min to 10 ml/min (Fig. 1 right). After being washed twice with the MES-Na buffer, cells were resuspended in accordance with buffers at a density of 10^5 – 10^6 cells/ml. Resuspended cells were immediately introduced into the channel slide and allowed to settle and adhere for 10 min. The surface density was approximately 50 cells/mm², corresponding to a less than 1% surface coverage. No hydrodynamic interaction between adjacent cells was detected during the experiments.

The action of shear flow on the cell adhering to the substrate is determined by the hydrodynamic forces exerted on the cell. When the Reynolds number is small, inertial effects can be neglected. In a laminar flow, the net force and torque exerted on an adhering cell, considering it as an elastic solid, are proportional to the wall shear stress. Given the geometry of the channels (see Sec. II E), the shear stress is given by

$$\sigma = \frac{6\eta D}{wh^2},$$

where D is the flow rate, η is the dynamic viscosity of the fluid, w is the width of the channel, and h is the height of the channel.

C. Analysis of shearotactic response

The centroid positions, (x_i, y_i) , of individual cells in the (xy) -bottom plane of the channel slide were extracted from the series of images depending on the frame rate chosen. The

instantaneous velocity, (v_{xi}, v_{yi}) , is obtained through first-order finite differences. The instantaneous velocity along the x -axis is calculated from the following formula:

$$v_x(t_i) = \frac{x(t_{i+1}) - x(t_i)}{t_{i+1} - t_i},$$

where $x(t_i)$ denotes the cell position in the i -th frame at time t_i along the x -axis, and $v_x(t_i)$ denotes the velocity component, at instant t_i , in the direction of the x -axis, which is systematically taken parallel to the mechanostimulus direction. The instantaneous velocity component along the y -direction is computed in a similar way by simply replacing x by y . The instantaneous angle θ_i is defined as the angle between the velocity vector and the horizontal axis (x -axis), classically measured in counterclockwise direction. Practically, this process—simply amounting to a first-order time derivative—for obtaining the velocity and speed of cells is known to amplify the noise and fluctuations in the cell position. Consequently, the velocity was obtained with an 11-point Savitzky and Golay differentiation filter effectively smoothing the high-frequency fluctuations. The application of this differentiation filter was found to have very negligible effect on the average velocity components and average speed.

Similar to the study of other taxis, our measure of the shearotactic efficiency comprises two components: (i) the shearotactic directionality (S_d) of the cells measured by $\langle \cos \theta_i \rangle$, θ_i being the angle between the instantaneous cell velocity v_i and the direction of the shear flow, arbitrarily chosen as the positive x -direction, and (ii) the shearotactic index (S_i), defined as the ratio of the distance traveled in the direction of the flow to the total length of the cell migration path during the same period. Cells moving randomly have a shearotactic directionality of 0, while cells moving straight along the flow have a directionality of 1; cells moving straight against the flow have a directionality of -1 .

D. Shear-flow induced cellular detachment

Cells were suspended in the MES-Na buffer with different levels of extracellular soluble calcium and injected into different channels. Cells were spread at a density of 100 cells/mm², giving a fraction of surface occupied of 3%, on the bottom surface of the channel and allowed to settle and adhere for 10 min. Given that the surface coverage of cells is below 7%, hydrodynamic interactions between cells can be neglected.⁴⁶ The cells were then subjected to a shear stress of magnitude $\sigma = 1$ Pa in selected buffers. This choice for the value of σ is based on the reported value for the adhesion strength being around 1 Pa.⁴ Video recording was started after cells were exposed to the shear flow for 30 s. The remaining fraction of cells was then calculated after a 10-min exposition to this shear flow.

E. Substrate surfaces

We used hydrophobic and hydrophilic plastic channel slides (μ -slide VI 0.4 from ibidi) both having a width $w = 3.8$ mm, a height $h = 0.4$ mm, and a length $l = 17$ mm (see Fig. 1, left). The hydrophilic substrate surface is characterized by a contact angle of 15°, while the hydrophobic one has a contact angle of 100°. The hydrophobic surface is obtained with an uncoated polystyrene plastic surface, while the hydrophilic one is obtained through the so-called “ibiTreat” treatment, consisting in plasma cleaning of the polystyrene plastic surface. The third microfluidic channel considered is a glass channel (purchased from Translume and made of transparent fused silica glass) having a width $w = 0.3$ mm, a height $h = 0.3$ mm, and a length $l = 38$ mm. The rigidity of the plastic and glass channels are characterized by their Young’s modulus: approximately 1 GPa for the plastic microchannels from ibidi, and in the 50–90 GPa range for the glass microchannel from Translume. The glass channel was systematically washed with a mild detergent, followed by a concentrated NaOH solution (10 M) for 10 min, and then thoroughly rinsed with ethanol and distilled water, making it hydrophilic.

F. Statistical analysis

As already mentioned in the Introduction, our experimental setup (Fig. 1 right) permits direct visualization of transient responses of multiply seeded cells, thereby allowing for the simultaneous tracking of multiple independent cell responses. Our analysis of shearotactic motility is a statistical one, which is based on a quantification of the cellular responses of a statistically significant sample of cells. An indication of the size of these samples is given for each result.

It is well known that *Dictyostelium discoideum*'s basic motion can vary significantly from one set of experiment to another, even when using the same cell's strain and experimental protocol. To account for this, all results presented in this article were obtained from three distinct sets of experiment, which served to perform a classical bootstrapping resampling based on the generation of 100 bootstrap samples. The control of the statistical consistency was achieved by verifying that the standard deviation after resampling through the bootstrapping technique was the lower bound of all three standard deviations (SDs) for each experimental batch. The results of this statistical analysis take the form of probability density functions (PDF) or classical averages and associated SDs.

III. RESULTS AND DISCUSSION

A. Influence of extracellular calcium level on shearotactic cell guiding

We consider a wide range of extracellular calcium concentration from $10\ \mu\text{M}$ to $50\ \text{mM}$ for the study of shearotactic guiding of cells crawling on two different plastic substrates with hydrophobic and hydrophilic features (see Sec. II). Similarly to what we reported in Ref. 8, albeit extended to include the hydrophilic case, we obtain a clear optimal value for the calcium concentration with regard to both average cell speed and shearotactic efficiency (Fig. 2).

Figure 2 shows clearly the peak responses in terms of \mathcal{S}_d , \mathcal{S}_i and average in-flow velocity v_x all within a relatively narrow optimal range of $[\text{Ca}^{2+}]_{\text{ext}}$ for, respectively, the plastic hydrophobic and plastic hydrophilic substrates: $[\text{Ca}^{2+}]_{\text{ext}} \simeq 3\ \text{mM}$ for the hydrophobic and $[\text{Ca}^{2+}]_{\text{ext}} \simeq 10\ \text{mM}$ for the hydrophilic surface. The peak amplitudes are quantitatively distinct between the two surfaces with values for the hydrophobic surface 30% higher for all three measures (Table I). Figure 2 corresponds to cells being driven with a shearotactic signal of $\sigma = 0.18\ \text{Pa}$. Figs. 3 and 4 show that the features of directed migration for Dd cells are only very moderately affected by variations of σ around this value—in the $0 \leq \sigma \leq 0.5\ \text{Pa}$ range. In particular, the observed quantitative difference in the response on different substrates are consistent across this range of σ , e.g., for the cell speed (Fig. 3) and directionality (Fig. 4). Also, note the broader PDFs with varying shearotactic signals for cells crawling on hydrophobic surfaces as compared to hydrophilic ones. Such low shear stress values are considered for mainly two reasons: (i) to ensure persistence of directed migration associated with an almost negligible occurrence of cell-substrate detachment, and (ii) to reflect the known ability of cells to be driven *in vivo* by very low shearotactic stimuli.⁸

As already noted in Ref. 8, these results associated with the influence of soluble calcium on shearotactic guiding are remarkable as they seem to contradict the assumption of an independent regulation of speed and shearotactic efficiency (measured by shearotactic index and directionality).²⁴ This is further confirmed here for cells crawling on a hydrophilic plastic substrate. Moreover, an excess of calcium—beyond $50\ \text{mM}$ —totally hinders cellular migration as the speed tends toward zero regardless of the nature of the substrate (Fig. 2(c)). However, a full confirmation of the non-independent regulation of speed and shearotactic efficiency is beyond the scope of this study and would require a more thorough analysis, which could involve studying the evolution of the probability density function of cell speed with the soluble calcium concentration, with or without any shearotactic signal. Furthermore, additional experiments using wortmannin and LY294002 drugs, as was done in Ref. 7, could help shed some light on this issue of possible coupling in the regulation of speed and directionality.

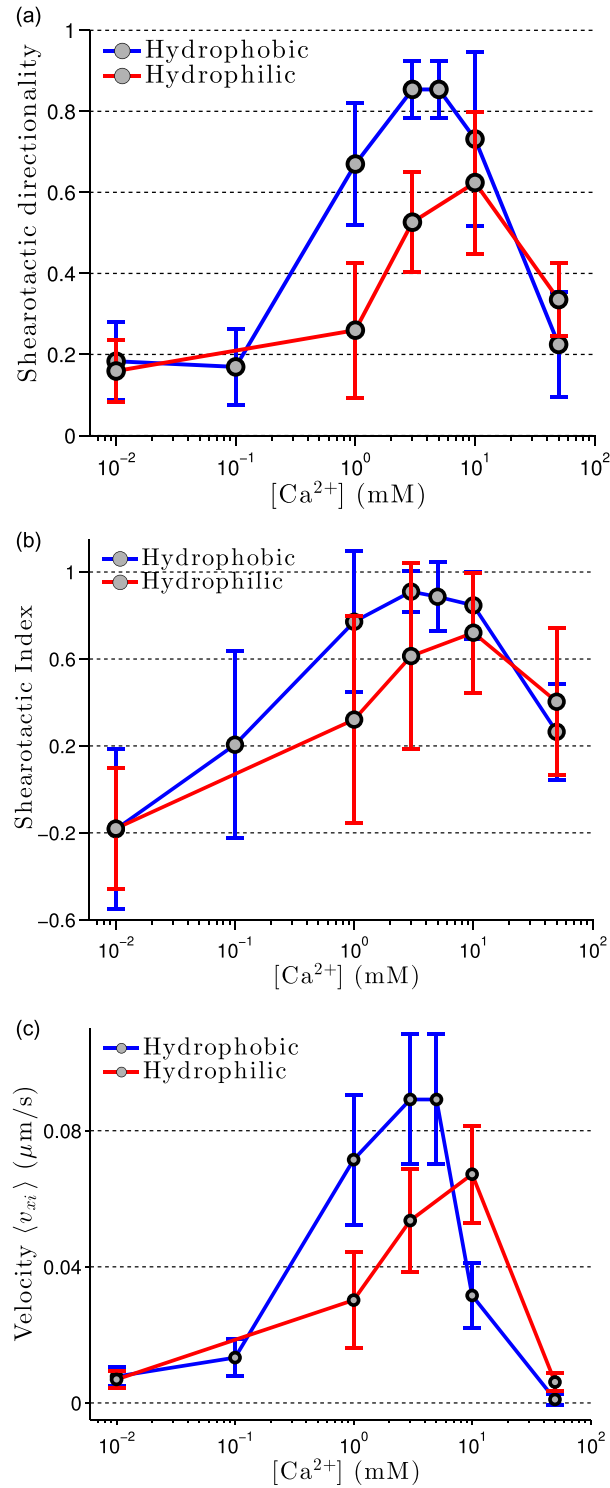


FIG. 2. (a) Shearotactic directionality S_d . (b) Shearotactic index S_i . (c) Average x -component of the cell velocity $\langle v_x \rangle$ for a shearotactic signal of magnitude $\sigma = 0.18$ Pa in the positive x direction. At both ends of the calcium concentration range considered, the shearotactic efficiency is extremely poor as attested by the values of S_d and S_i . A high shearotactic efficiency is achieved for calcium concentrations in the 1–10 mM range with both hydrophilic and hydrophobic substrates. For the speed, a clear maximum is attained for a concentration of 3 mM (hydrophobic) and 10 mM (hydrophilic). A log-scale is used for the calcium concentration on the horizontal axes. For each value of $[Ca^{2+}]_{\text{ext}}$, the averaging process is based on a population comprising between 60 and 135 (respectively 93 to 154) individual tracked cells for a duration of 1200 s and with a sampling time of 15 s on the hydrophobic (resp. hydrophilic) surface. The errorbars represent the SD (see Sec. II).

TABLE I. Values of the average (\pm SD) shearotactic directionality $\langle S_d \rangle$, average shearotactic index $\langle S_i \rangle$, and average cell speed $\langle v_i \rangle$ for a driving signal of magnitude $\sigma = 0.18$ Pa in the presence of a 3 mM extracellular calcium concentration. The averaging process is based on a population comprising the following number of individual tracked cells for a duration of 1200 s with a sampling time of 15 s: (i) 61 cells for the glass hydrophilic substrate, (ii) 135 for the plastic hydrophobic substrate, and (iii) 93 cells for the plastic hydrophilic substrate.

Substrate	$\langle S_d \rangle$	$\langle S_i \rangle$	$\langle v_i \rangle$ ($\mu\text{m/s}$)
Glass hydrophilic	0.665 ± 0.121	0.787 ± 0.087	0.063 ± 0.011
Plastic hydrophobic	0.837 ± 0.068	0.874 ± 0.089	0.114 ± 0.018
Plastic hydrophilic	0.514 ± 0.130	0.613 ± 0.406	0.084 ± 0.010

Another interesting element is to verify whether the presence of extracellular calcium has an effect on cell polarization. This effect is classically quantified by means of the roundness parameter defined as $\mathcal{R} = \text{perimeter}^2 / (4\pi \times \text{Area})$. For instance, a cell having a perfectly circular shape corresponds to a roundness of one, while an elliptical shape is associated with a roundness greater than the unity. In the absence of extracellular calcium, i.e., with the MES-Na buffer, the cell average roundness is 1.0994. With a buffer containing 3 mM of soluble calcium,

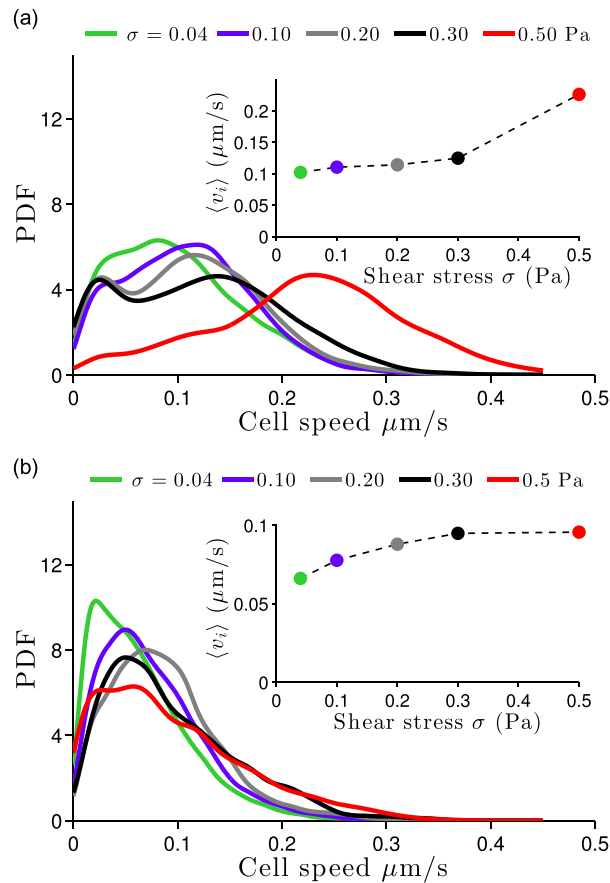


FIG. 3. Probability density function (PDF) of cell speed for five different magnitudes of the shearotactic signal, with the associated average speed vs. shear stress (inset). (a) Hydrophobic plastic substrate and (b) hydrophilic plastic substrate. For very low shear stress levels, in the $0.04 \leq \sigma < 0.3$ Pa range, the average cell speed increases very moderately with σ (inset). Between 124 to 262 ((a) hydrophobic substrate) and 121 to 291 ((b) hydrophilic substrate) cells were individually tracked for a duration of 600 s and a sampling time of 10 s was used to obtain the PDF and generate the averages. The extracellular calcium concentration is fixed at 3 mM. See Sec. II for details about the statistical analysis.

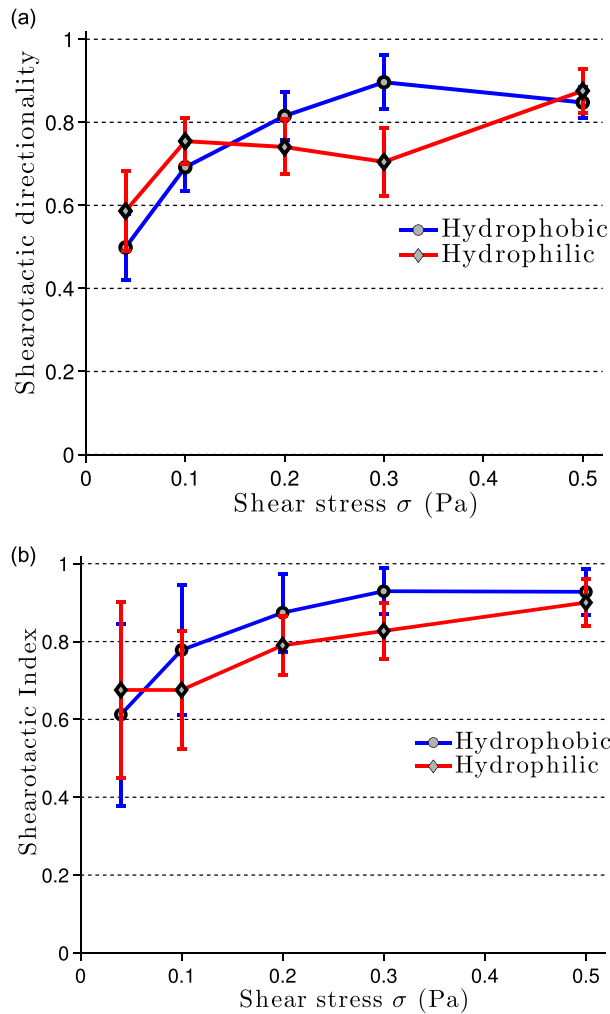


FIG. 4. (a) Shearotactic directionality \mathcal{S}_d versus shear stress σ and (b) shearotactic index \mathcal{S}_I versus σ , for a shearotactic signal pointing toward the positive x direction and with a concentration of extracellular calcium fixed at 3 mM. Between 124 to 262 ((a) hydrophobic substrate) and 121 to 291 ((b) hydrophilic substrate) cells were individually tracked for a duration of 600 s and a sampling time of 10 s was used to obtain the PDF and generate the averages. The errorbars represent the SD (see Sec. II).

a noticeable increase in the average cell roundness was observed, with $\mathcal{R} = 1.2337$. This shows that the presence of calcium in the buffer has a non-negligible effect on cell polarization.

The present study reveals two new and very important facts regarding the influence of the substrate. First, in the absence of extracellular soluble calcium, directed migration occurs with approximately the same, much reduced, speed (Fig. 2(c)), and very low shearotactic efficiency (Figs. 2(a) and 2(b)) on both the hydrophilic and hydrophobic plastic substrates. Second, with soluble calcium levels in the range similar to those typically encountered in soil solutions (concentrations of free Ca^{2+} commonly between 3.4 and 14 mM (Ref. 42)), the directed migration is optimal yet noticeably different for different substrates. Table II quantifies the differences in the shearotactic measures at a fixed extracellular calcium concentration $[\text{Ca}^{2+}]_{\text{ext}} = 3$ mM for the three substrates we tested (see Fig. 5). Table II reports the differences in the optimal shearotactic measures over the wide range of calcium concentrations considered in this study—from 10 μM to 50 mM. The substantive and consistent differences in the shearotactic measures for different physicochemical substrate properties offer an effective means for discriminating such surface properties using a population of mechanosensitive and guidable cells, such as Dd and neutrophils for instance.

TABLE II. Values of the optimal (\pm SD) shearotactic directionality $\langle S_d \rangle_{\text{opt}}$, optimal shearotactic index $\langle S_i \rangle_{\text{opt}}$, and optimal cell speed $\langle v_i \rangle_{\text{opt}}$, over the very wide range of extracellular calcium concentration considered in this study, and for a driving signal of magnitude $\sigma = 0.18$ Pa. The averaging process is based on a population comprising the following number of individual tracked cells for a duration of 1200 s with a sampling time of 15 s: 135 for the plastic hydrophobic substrate, and 121 cells for the plastic hydrophilic substrate.

Substrate	$\langle S_d \rangle_{\text{opt}}$	$\langle S_i \rangle_{\text{opt}}$	$\langle v_i \rangle_{\text{opt}}$ ($\mu\text{m/s}$)
Plastic hydrophobic	0.837 ± 0.068	0.874 ± 0.089	0.114 ± 0.018
Plastic hydrophilic	0.611 ± 0.141	0.642 ± 0.398	0.093 ± 0.015

These results further stress the pivotal role played by extracellular calcium in relation with directed migration.^{8,24,40,42,43} They also help reconcile some apparent inconsistencies in reports related to cellular migration of Dd cells over different surfaces.^{8,21,24,47}

B. Influence of extracellular calcium levels on cell-substrate adhesion

Given the known relationship between adhesion and motility, and the very marked influence of extracellular calcium on directed motility over different substrates, we now consider the influence of calcium on adhesion. The same wide range of soluble calcium concentrations, from $10 \mu\text{M}$ to 50mM , is considered so as to extend previous studies²⁴ of shearotaxis with lower calcium levels ($<1 \text{mM}$) with a single type of substrate. Among the many possible ways of measuring adhesion,⁴⁸ we choose the most natural method given our focus on cellular shearotaxis, namely, shear-flow detachment.⁴⁶ Specifically, we indirectly quantify the adhesion strength through the remaining fraction of cells adhering to the substrate after subjecting a given population of cells to a shear flow of magnitude $\sigma = 1 \text{Pa}$ for a fixed duration of 10 min (see Sec. II), thereby placing us in the steady-state regime of the kinetics of detachment.⁴⁶ Although this approach does not yield an actual direct measurement of the adhesion strength, it provides an indirect yet precise and useful means of comparing cellular adhesion under different environmental conditions—nature of the substrate and extracellular calcium levels in our case.

Interestingly, we find that the adhesion strength is minimal for all three substrates at the calcium concentration of 3mM (Fig. 6). This value is the one for which shearotactic motility was found to be optimal in the hydrophobic case, and close to optimal with the plastic hydrophilic substrate. To the best of our knowledge, this clear reduction of the adhesion strength in a fairly narrow range $0.5\text{--}10 \text{mM}$ of $[\text{Ca}^{2+}]_{\text{ext}}$ accompanied by a marked minimum, regardless of the nature of the substrate, has never been reported before for Dd. As with the earlier

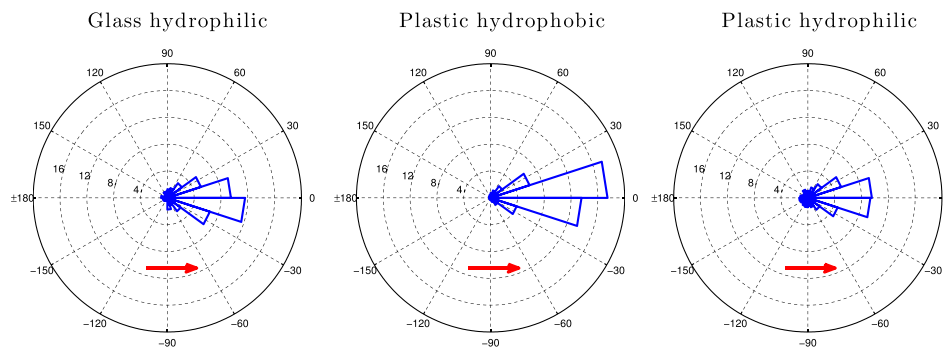


FIG. 5. Influence of substratum nature on cell directionality. The polar histograms demonstrate distribution of angles of net migration vectors for cell populations comprising the following number of individual tracked cells for a duration of 1200 s with a sampling time of 15 s, and for a driving signal of magnitude $\sigma = 0.18$ Pa in the presence of a 3mM extracellular calcium concentration: (i) 61 cells for the glass hydrophilic substrate, (ii) 135 for the plastic hydrophobic substrate, and (iii) 93 cells for the plastic hydrophilic substrate. We observe a noticeable directional bias in the direction of the shearotactic stimuli given by the red arrow. In all polar histograms, 20 equally spaced angular bins are considered.

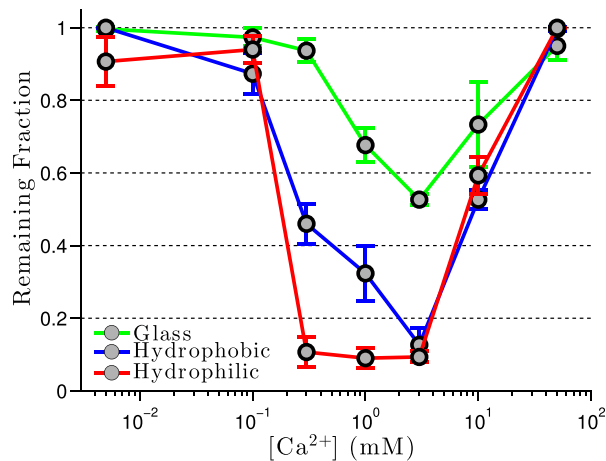


FIG. 6. Fraction of cells remaining adhered to the substrate for different soluble calcium concentration in the buffer, for three different substrates: plastic hydrophilic, plastic hydrophobic, and glass hydrophilic. A log-scale is used for the calcium concentration on the horizontal axis, and for each value of $[Ca^{2+}]_{ext}$ the averaging process is based on a set of three independent experiments, each involving at least 300 initially adhesive cells, subjected to a shear flow of magnitude 1 Pa over 600 s. The errorbars represent the SD (see Sec. II).

shearotactic motility indices, we see consistent quantitative differences in the magnitudes of the adhesion measure for different substrates, for instance, at $[Ca^{2+}]_{ext} = 3$ mM, the remaining fraction of cells adhering to the glass hydrophilic substrate is over 5 times that for plastic substrates (Fig. 6). At $[Ca^{2+}] = 1$ mM, the value for the hydrophobic plastic surface is over 3 times that of the hydrophilic plastic surface (Fig. 6).

The results shown in Fig. 6 are notable in several ways. First, they provide yet another evidence of the biphasic effect of cell-substratum adhesion on migration speed.¹ As already mentioned, the effectiveness of the haptokinetic migration of Dd requires a fine balance between the adhesion rate at the front of the cell and the de-adhesion rate at its rear. The comparison of our results for the glass hydrophilic and plastic hydrophilic substrates (i.e., for different values of the rigidity of the substrate) is quite revealing in that respect. Indeed, for the substrate having the highest rigidity, namely, the glass substrate, the levels of substrate adhesion are substantially higher as compared to those with the plastic substrate, and in the presence of 3 mM of extracellular calcium (Fig. 6). These higher levels of adhesion for the glass substrate, in turn, impede the de-adhesion process at the rear of the cell, which explains the reduced average cell speed on glass as compared to the plastic hydrophilic substrate (Table I, in the presence of 3 mM of extracellular calcium). These results also reveal that the rigidity of the substrate contributes to the regulation of cellular adhesion for Dd cells. Second, they uncover the existence of a clear relationship between directionality and adhesion. For low calcium concentrations, $[Ca^{2+}]_{ext} < 0.1$ mM, and high ones, $[Ca^{2+}]_{ext} > 50$ mM, the measured high levels of adhesion (Fig. 6) coincide with baseline levels of shearotactic directionality (Fig. 2(a)). Conversely, with calcium concentrations between 1 mM and 10 mM, reduced levels of adhesion (Fig. 6) are associated with maximum levels of \mathcal{S}_d and \mathcal{S}_i (Fig. 2(a)). Third, if soluble calcium concentration is not in the narrow range 0.5 mM to 10 mM, the cell-substrate adhesion strength remains elevated, irrespective of the physicochemical properties of the substrate, which was shown in Fig. 3 to impair shearotactic migration. This third point is extremely important as it reveals that calcium plays a pivotal *indirect* role in the active regulation of adhesion. Indeed, calcium is not known to be a chemical element directly necessary for the establishment of adhesion focal points. Finally, the adhesion strength varies significantly for substrates with different physicochemical properties, thereby emphasizing the natural adaptive character of cellular adhesion in Dd cells.

Given the recent accumulation of evidences of a calcium-based mechanosensitivity in Dd,^{24,40,41} we are led to suspect that the observed active regulation of adhesion associated with

optimal directed migrations finds its origin in the mechanosensitive capability of the cells. The significant variability in results for cells on different substrates could therefore be associated with different mechanosensitive affinity of the cell to substrates having varying physicochemical properties.

C. Cell-substrate adhesion with knocked down mechanosensation

To test the possible implication of cellular mechanosensation onto the active regulation of cell-substrate adhesion, we consider knocking down the most effective elements of the mechanosensory apparatus, namely, the MSCs.³⁷ Lima *et al.*⁴¹ have recently revealed the pivotal role played by the MSC PKD2 in the mechanotactic behavior of Dd cells. To achieve this, we treat cell populations with gadolinium (Gd^{3+}), which is commonly used to block MSCs.⁴⁹ On Dd cells, gadolinium has already been shown to significantly impede the random migration of wild type cells,⁴⁰ chemotactic migration,⁴⁰ and shearotactic migration.²⁴ However, no report of the effects of gadolinium on cellular adhesion exists.

First, we test the ability of cells in recovering motility after having its stretch-activated channels blocked by Gd^{3+} for 10 min. After 10 min, the gadolinium ions were washed away with a MES- Ca^{2+} buffer, and after less than 5 min cell motility was fully recovered with average cell speed in the 5–10 $\mu\text{m}/\text{min}$. Subsequently, we investigate the effects of increasing the concentration of Gd^{3+} on the strength of cellular adhesion—the remaining fraction is again used as a proxy for this quantity. Specifically, we focus our attention on the particular case of the plastic hydrophobic substrate since it has shown to yield the most effective shearotactic migration (Table I and Fig. 5) and regulation of adhesion (Fig. 6) at the optimal calcium concentration of 3 mM. Our results show that with increasing levels of gadolinium from $[Gd^{3+}] = 1 \mu\text{M}$ to $[Gd^{3+}] = 100 \mu\text{M}$ —corresponding to increasing inhibition of MSCs and thereby decreasing mechanosensitive capability—the strength of adhesion increases monotonously (Fig. 7). Time lapse movies of these cellular detachment experiments in the presence of 3 mM of calcium and under a shear flow of magnitude 1 Pa are available in movies S1–S3 in the supplementary material.⁵¹ These observations thus confirm the central role played by calcium-based mechanosensitivity on the active regulation of cellular adhesion. The maximum concentration of gadolinium considered here, $[Gd^{3+}] = 100 \mu\text{M}$, has previously been shown^{24,40} to be sufficient to fully block all MSCs and therefore totally disrupt calcium-based mechanosensation. We also report that at $[Gd^{3+}] = 100 \mu\text{M}$, the influence of calcium levels on the strength of cellular adhesion revealed in Fig. 6 completely disappears (Fig. 8). This fact further confirms

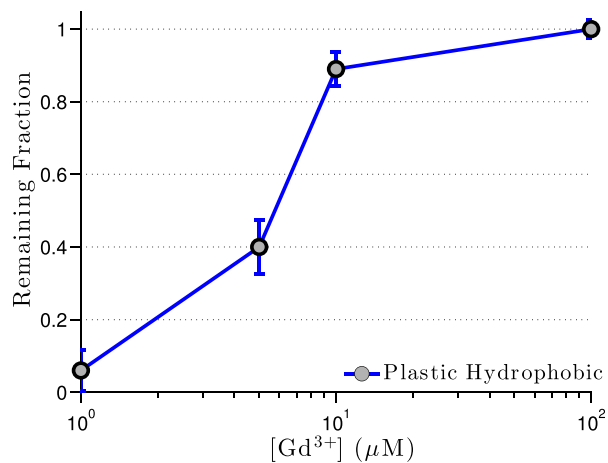


FIG. 7. Fraction of cells remaining adhered to the substrate versus soluble gadolinium (Gd^{3+}) concentration in the buffer for the plastic hydrophobic substrate. Calcium level is set at 3 mM. A log-scale is used for the Gd^{3+} concentration on the horizontal axis. For each value of $[Gd^{3+}]$, the averaging process is based on a population comprising at least 200 initially adhesive cells, which are subjected to a shear flow of magnitude 1 Pa over 600 s. The errorbars represent the SD (see Sec. II).

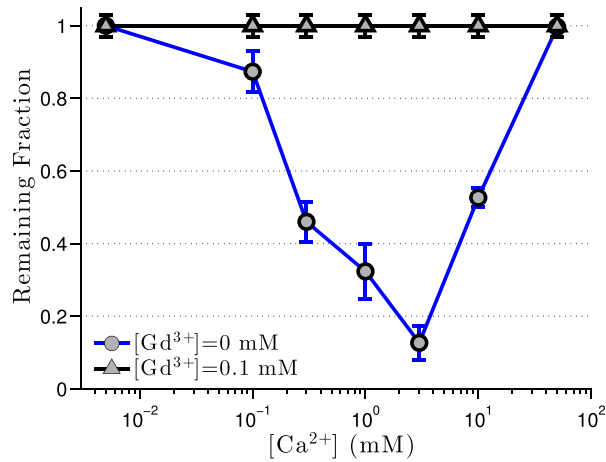


FIG. 8. Fraction of cells remaining adhered to the substrate versus soluble calcium concentration in the buffer for the plastic hydrophobic substrate. A high level of soluble gadolinium, $[\text{Gd}^{3+}] = 100 \mu\text{M}$, is considered and compared to the same case in the absence of gadolinium. A log-scale is used for the calcium concentration on the horizontal axis. For each value of $[\text{Ca}^{2+}]_{\text{ext}}$, the averaging process is based on a population comprising at least 300 initially adhesive cells, which are subjected to a shear flow of magnitude 1 Pa over 600 s.

TABLE III. Values of the average (\pm SD) shearotactic directionality $\langle S_d \rangle$, average shearotactic index $\langle S_i \rangle$, and average cell speed $\langle v_i \rangle$ for a driving signal of magnitude $\sigma = 0.18$ Pa in the presence of a 3 mM extracellular calcium concentration for the plastic hydrophobic substrate. The averaging process is based on a population comprising at least 138 individual tracked cells for a duration of 600 s with a sampling time of 10 s.

$[\text{Gd}^{3+}](\mu\text{M})$	$\langle S_d \rangle$	$\langle S_i \rangle$	$\langle v_i \rangle (\mu\text{m/s})$
0	0.841 ± 0.071	0.898 ± 0.095	0.109 ± 0.015
5	0.602 ± 0.061	0.665 ± 0.066	0.061 ± 0.009
10	0.518 ± 0.049	0.588 ± 0.049	0.060 ± 0.009
100	0.073 ± 0.011	0.098 ± 0.008	0.021 ± 0.006

the necessity of calcium-based mechanosensation for Dd cells to effectively regulate adhesion regardless of the extracellular calcium concentration.

D. Shearotactic motility with knocked down mechanosensation

To close the loop on our study of the triadic coupling between motility, cell-substrate adhesion and mechanosensitivity, we now consider the effects of reduced calcium-based mechanosensation on directed motility. To this aim, we increased the concentration of gadolinium in the buffer all the way to $[\text{Gd}^{3+}] = 100 \mu\text{M}$. We again focused on the particular case of the plastic hydrophobic substrate for the same reasons as before. The shearotactic efficiency—measured by S_d and S_i —is significantly impaired with increasing amounts of Gd^{3+} (Table III). This result could have been anticipated since: (i) such a mechanotactic behavior requires effective mechanosensation and (ii) increasing levels of Gd^{3+} have been shown to impair the active regulation of cell-substrate adhesion (Fig. 7), which is a key to the effectiveness of migration. This latter point also explains the sharp reduction in average cell speed (Table III) with increasing amounts of gadolinium.

We can now conclude that effective directed migration requires actively regulated cell-substrate adhesion, which in turn necessitates effective cellular mechanosensation.

IV. CONCLUSIONS

In their natural environment, *Dictyostelium* cells adhere to extracellular matrix proteins in order to translocate, while *in vitro* they have been shown to migrate over and adhere to plain or

coated materials of varying rigidity and topography. However, many quantitative measurements of adhesive properties—kinetics of cellular detachment from the substrate or threshold shear stress for instance—and migration properties—speed and directionality—heretofore reported in the literature are not always consistent.^{7,8,20,21,24,44,46,48,50} Beyond the inevitable issue of biological variability, these apparent inconsistencies are rooted in the intricate coupling between the large number of control parameters associated with: (i) the cell itself—primarily strain and growth phase, (ii) the substratum—rigidity, topography and the possible chemical coating, (iii) the fluid environment between the cell and substratum—shear stress and soluble chemicals, e.g., 3',5'-cyclic adenosine monophosphate (cAMP) or extracellular calcium, and (iv) the presence or not of a driving signal of either chemical or mechanical origin. The triadic coupling among motility/adhesion/mechanosensation elucidated in this study helps substantially in reconciling these apparently inconsistent reports.^{7,8,20,21,24,44,46,48,50} Specifically, with too little or too much calcium, mechanosensation is impaired leading to ineffective regulation of adhesion and thereby hindering motility. This is particularly true for experiments lacking calcium in the extracellular environment. The present study shows that in the absence of calcium, measures of adhesion and motility with vastly different substrates are approximately the same. Even with appropriate calcium levels, measures of adhesion and motility show clear differences for different substrate properties. This result is consistent with the fact that amoeboid cells are known to be highly adaptable to their environment and to develop effective migration capabilities over physicochemically different substrates. Our study therefore reveals the key role played by mechanosensation in the inherent adaptability to their environment of *Dictyostelium* cells.

Finally, we propose that this adaptive behavior of Dd cells to substrates having varying physicochemical properties could be used for the development of novel surface analysis methods. The essence of this method would consist of using the mechanobiological ability of cells to probe a substrate at the nanometer scale. Through quantitative measurements of adhesion and stimuli-driven motility of large populations of mechanosensitive cells, this method could provide efficacious means of discriminating between surfaces having a certain level of variations in their physical and/or chemical properties.

ACKNOWLEDGMENTS

This work was supported by the SUTD–MIT International Design Centre (IDC) Grant No. IDG31400104 (X.Z. and R.B.).

- ¹P. Friedl, S. Borgmann, and E.-B. Bröcker, *J. Leukocyte Biol.* **70**, 491–509 (2001), available online at <http://www.jleukbio.org/content/70/4/491.full.html>.
- ²J. Renkawitz, K. Schumann, M. Weber, T. Lämmermann, H. Pflicke, M. Piel, J. Polleux, J. Spatz, and M. Sixt, *Nat. Cell Biol.* **11**, 1438–1443 (2009).
- ³C. L. Manahan, P. A. Iglesias, Y. Long, and P. N. Devreotes, *Annu. Rev. Cell Dev. Biol.* **20**, 223–253 (2004).
- ⁴H. Delanoë-Ayari, S. Iwaya, Y. T. Maeda, J. Inose, C. Rivière, M. Sano, and J. Rieu, *Cell Motil. Cytoskeleton* **65**, 314–331 (2008).
- ⁵R. H. Kessin, *Dictyostelium: Evolution, Cell Biology, and the Development of Multicellularity* (Cambridge University Press, Cambridge, UK, 2001).
- ⁶A. Müller-Taubenberger, A. Kortholt, and L. Eichinger, *Eur. J. Cell Biol.* **92**, 45–53 (2013).
- ⁷E. Décavé, D. Rieu, J. Dalous, S. Fache, Y. Bréchet, B. Fourcade, M. Satre, and F. Brückert, *J. Cell Sci.* **116**, 4331–4343 (2003).
- ⁸X. Zhu, R. Bouffanais, and D. K. P. Yue, *PLoS One* **9**, e105406 (2014).
- ⁹A. Makino, E. R. Prossnitz, M. Bünemann, J. M. Wang, Y. Yao, and G. W. Schmid-Schönbein, *Am. J. Physiol.: Cell Physiol.* **290**, C1633–C1639 (2006).
- ¹⁰L. A. Smith, H. Aranda-Espinoza, J. B. Haun, and D. A. Hammer, *Biophys. J.* **92**, 632–640 (2007).
- ¹¹G. Charras and E. Paluch, *Nat. Rev. Mol. Cell Biol.* **9**, 730–736 (2008).
- ¹²M. L. Lombardi, D. A. Knecht, M. Dembo, and J. Lee, *J. Cell Sci.* **120**, 1624–1634 (2007).
- ¹³Y. Iwadate and S. Yumura, *J. Cell Sci.* **121**, 1314–1324 (2008).
- ¹⁴K. S. K. Uchida and S. Yumura, *J. Cell Sci.* **117**, 1443–1455 (2004).
- ¹⁵L. Eichinger, J. A. Pachebat, G. Glockner, M. A. Rajandream, R. Sugang *et al.*, *Nature* **435**, 43–57 (2005).
- ¹⁶S. Cornillon, E. Pech, M. Benghezal, M. Ravel, E. Gaynor, F. Letourneur, F. Brückert, and P. Cosson, *J. Biol. Chem.* **275**, 34287–34292 (2000).
- ¹⁷P. Fey, S. Stephens, M. A. Titus, and R. L. Chisholm, *J. Cell Biol.* **159**, 1109–1119 (2002).
- ¹⁸S. Cornillon, L. Gebbie, M. Benghezal, P. Nair, S. Keller, B. Wehrle-Haller, S. J. Charette, F. Brückert, F. Letourneur, and P. Cosson, *EMBO Rep.* **7**, 617–621 (2006).
- ¹⁹S. Cornillon, R. Froquet, and P. Cosson, *Eukaryotic Cell* **7**, 1600–1605 (2008).

- ²⁰W. F. Loomis, D. Fuller, E. Gutierrez, A. Groisman, and W.-J. Rappel, *PLoS One* **7**, e42033 (2012).
- ²¹C. McCann, E. C. Rericha, C. Wang, W. Losert, and C. A. Parent, *PLoS One* **9**, e87981 (2014).
- ²²P. A. Janmey and C. A. McCulloch, *Annu. Rev. Biomed. Eng.* **9**, 1–34 (2007).
- ²³J. Árnadóttir and M. Chalfie, *Annu. Rev. Biophys.* **39**, 111–137 (2010).
- ²⁴S. Fache, J. Dalous, M. Engelund, C. Hansen, F. Chamaroux, B. Fourcade, M. Satre, P. Devreotes, and F. Brückert, *J. Cell Sci.* **118**, 3445–3457 (2005).
- ²⁵A. D. Bershadsky, N. Q. Balaban, and B. Geiger, *Annu. Rev. Cell Dev. Biol.* **19**, 677–695 (2003).
- ²⁶A. Bershadsky, M. Kozlov, and B. Geiger, *Curr. Opin. Cell Biol.* **18**, 472–481 (2006).
- ²⁷C. Moares, Y. Sun, and C. A. Simmons, *Integr. Biol.* **3**, 959–971 (2011).
- ²⁸V. Vogel and M. Sheetz, *Nat. Rev. Mol. Cell Biol.* **7**, 265–275 (2006).
- ²⁹C. M. Lo, H. B. Wang, M. Dembo, and Y. L. Wang, *Biophys. J.* **79**, 144–152 (2000).
- ³⁰D. Arcizet, S. Capito, M. Gorelashvili, C. Leonhardt, M. Vollmer, S. Youssef, S. Rappl, and D. Heinrich, *Soft Matter* **8**, 1473–1481 (2012).
- ³¹M. M. Stevens and J. H. George, *Science* **310**, 1135–1138 (2005).
- ³²J. Wu, Z. Mao, H. Tan, L. Han, T. Ren, and C. Gao, *Interface Focus* **2**, 337–355 (2012).
- ³³H.-D. Kim and S. R. Peyton, *Integr. Biol.* **4**, 37–52 (2012).
- ³⁴M. Singh, C. Berkland, and M. S. Detamore, *Tissue Eng., Part B* **14**, 341–366 (2008).
- ³⁵C. Moares, G. Mehta, S. C. Leshner-Perez, and S. Takayama, *Ann. Biomed. Eng.* **40**, 1211–1227 (2012).
- ³⁶E. S. Place, N. D. Evans, and M. M. Stevens, *Nat. Mater.* **8**, 457–470 (2009).
- ³⁷S. Sukharev and F. Sachs, *J. Cell Sci.* **125**, 3075–3083 (2012).
- ³⁸R. Bouffanais, J. Sun, and D. K. P. Yue, *Phys. Rev. E* **87**, 052716 (2013).
- ³⁹T. Ursell, J. Kondev, D. Reeves, P. A. Wiggins, and R. Phillips, *Mechanosensitive Ion Channels* (Springer-Verlag, Berlin, 2008), Chap. 2, pp. 37–70.
- ⁴⁰M. L. Lombardi, D. A. Knecht, and J. Lee, *Exp. Cell Res.* **314**, 1850–1859 (2008).
- ⁴¹W. C. Lima, A. Vinet, J. Pieters, and P. Cosson, *PLoS One* **9**, e88682 (2014).
- ⁴²D. F. Lusche, D. Wessels, and D. R. Soll, *Cell Motil. Cytoskeleton* **66**, 567–587 (2009).
- ⁴³A. Scherer, S. Kuhl, D. Wessels, D. F. Lusche, B. Raisley, and D. R. Soll, *J. Cell Sci.* **123**, 3756–3767 (2010).
- ⁴⁴J. Dalous, E. Burghardt, A. Müller-Taubenberger, F. Brückert, G. Gerisch, and B. Bretschneider, *Biophys. J.* **94**, 1063–1074 (2008).
- ⁴⁵D. J. Watts and J. M. Ashworth, *Biochem. J.* **119**, 171–174 (1970).
- ⁴⁶E. Décavé, D. Garrivier, Y. Bréchet, B. Fourcade, and F. Brückert, *Biophys. J.* **82**, 2383–2395 (2002).
- ⁴⁷I. Weber, E. Wallraff, R. Albrecht, and G. Gerisch, *J. Cell Sci.* **108**, 1519–1530 (1995), available online at <http://jcs.biologists.org/content/108/4/1519.short>.
- ⁴⁸F. Brückert, E. Décavé, D. Garrivier, P. Cosson, Y. Bréchet, B. Fourcade, and M. Satre, *J. Muscle Res. Cell Motil.* **23**, 651–658 (2002).
- ⁴⁹X. C. Yang and F. Sachs, *Science* **243**, 1068–1071 (1989).
- ⁵⁰P. Rupprecht, L. Golé, J.-P. Rieu, C. Vézy, R. Ferrigno, H. C. Mertani, and C. Rivière, *Biomicrofluidics* **6**, 014107 (2012).
- ⁵¹See supplementary material at <http://dx.doi.org/10.1063/1.4931762> for: (i) Movie S1 for $[Gd^{3+}] = 1 \mu M$; (ii) Movie S2 for $[Gd^{3+}] = 10 \mu M$; and (iii) Movie S3 for $[Gd^{3+}] = 100 \mu M$.